

AC losses in macroscopic thin-walled superconducting niobium cylinders

M. I. Tsindlekht,^{1,*} V. M. Genkin,¹ I. Felner,¹ F. Zeides,¹ N. Katz,¹ Š. Gazi,² Š. Chromik,² and O. V. Dobrovolskiy³

¹The Racah Institute of Physics, The Hebrew University of Jerusalem, 91904 Jerusalem, Israel

²The Institute of Electrical Engineering SAS, Dúbravská cesta 9, 84104 Bratislava, Slovakia

³Faculty of Physics, University of Vienna, Boltzmanngasse 5, 1090 Vienna, Austria

(Dated: June 23, 2021)

Measurements of the ac response represent a widely-used method for probing the properties of superconductors. In the surface superconducting state (SSS), increase of the current beyond the surface critical current I_c leads to breakdown of SSS and penetration of external magnetic field into the sample bulk. An interesting free-of-bulk system in SSS is offered by thin-walled superconducting cylinders. The critical state model (CSM) asserts the ac susceptibility χ to exhibit jumps as a function of the external ac field amplitude H_{ac} , because of the periodic destruction and restoration of SSS in the cylinder wall. Here, we investigate experimentally the low-frequency (128-8192 Hz) ac response of thin-walled superconducting cylinders in superimposed dc and ac magnetic fields applied parallel to the cylinder axis. Distinct from the CSM predictions, experiments reveal that χ is a smooth function of H_{ac} . For the explanation of our observations we propose a phenomenological model of partial penetration of magnetic flux (PPMF). The PPMF model implies that after a restoration of the superconducting state, the magnetic flux inside and outside the cylinder are not equal, and the value of the penetrating flux is random for each penetration. This model fits very well to the experimental data on the temperature dependence of the first-harmonic χ_1 at any H_{ac} and dc field magnitude. However, in a certain temperature range the values of physical parameters deduced within the framework of the PPMF model are questionable.

I. INTRODUCTION

The ac magnetic response contains essential information about the properties of superconductors. Peculiarities of the ac response of conventional and high- T_c superconductors have been a matter of extensive research [1–6]. Low- T_c superconductors were investigated a long time ago [1–3] and revealed an absorption maximum at the transition upon variation of temperature and dc magnetic field. The ac response of high- T_c superconductors exhibits similar features [4–6]. However, the physical reasons for this behavior remain unclear. The first Maxwell-Strongin model [1] assumed the existence of microscopic superconducting filaments that underlaid an increase of the normal conductivity [7]. A more general eddy current model [8] suggested that the normal conductivity increases due to the appearance of superconducting inclusions, which leads to an absorption maximum near T_c . However, a further analysis based on the two-fluid model did not confirm the existence of the absorption maximum in the ac response [9]. On the other hand, the BCS theory [10] asserts an increase in the normal conductivity at low frequencies due to the singularity in the density of states [9]. This dissipative conductivity has a logarithmic singularity and appears only in a vanishingly narrow temperature interval [9].

In a magnetic field applied parallel to the sample surface, an absorption maximum was observed in the surface superconducting state (SSS), i.e., in fields H_0 exceeding the second critical field H_{c2} [2, 3, 11, 12]. It is known that in the presence of a transport current I , SSS is stable only if $I < I_c$, where I_c is the surface critical current [13–15]. If at a certain instantaneous value of the external field the surface current reaches the critical value, a further increase of the field leads to destruction of SSS. The breakdown of SSS is followed by the

penetration of external magnetic field into the sample bulk. The critical state model (CSM) [2, 16] neglects this SSS instability and assumes that SSS at $I = I_c$ is stable. It was suggested that if the difference between the applied magnetic field $H_{ext}(t) = H_0 + H_{ac} \sin(\omega t)$ and the magnetic field in the bulk $H_{int}(t)$ reaches a certain critical value, the current in the entire surface sheath becomes equal to I_c . Here, $H_0 > H_{c2}$ and H_{ac} are the magnitude of the dc field and the amplitude of the ac field, respectively. In this case H_{int} follows the applied field H_{ext} with some delay, i.e. $H_{int} = H_{ext} \mp H_c$. Here, the signs of the surface critical field H_c correspond to increasing and decreasing external field, respectively. This assumption implies that if $|H_{ext} - H_{int}| < H_c$, the surface current is a linear function of H_{ext} and H_{int} does not depend on H_{ext} [2, 17, 18]. In this approximation, during a slow course of the ac cycle at a constant H_0 , a minor magnetization loop $H_{int}(H_{ext}(t))$ looks as shown in Fig. 1. In Fig. 1 and in what follows, h_{int} and h_{ext} denote the respective dimensionless quantities.

An interesting application of the CSM is discussed in [19], where the CSM was applied for analyzing the electromagnetic response of macroscopic thin-walled cylinders in trans-

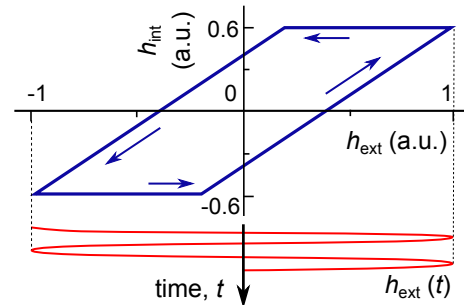


FIG. 1. Minor magnetization loop $h_{in}(h_{ext}(t))$ of a superconducting sample during a slow course of the ac cycle for the ratio $h_c/h_{ac} = 0.4$.

* Corresponding author: mtsindl@mail.huji.ac.il

verse magnetic fields [19]. In such cylinders, the thickness $d \approx \lambda \gg \xi$, with λ being the magnetic penetration depth and ξ the superconducting coherence length. The essential prediction of this theoretical work [19] is a jump in the ac susceptibility of thin-walled superconducting cylinders as a function of the ac excitation amplitude.

In the last decade, superconducting thin-walled cylinders of (sub-)micrometer diameters have attracted great attention. This interest is, in particular, caused by the exploration of topological transitions in the patterns of screening currents [20], Aharonov-Bohm oscillations [21], and the intricate dynamics of vortices [22, 23] and phase slips of the superconducting order parameter [24–26]. At the same time, macroscopic thin-walled cylinders are scarcely studied, while exhibiting such interesting phenomena such as giant jumps of magnetic flux in longitudinal fields [27]. It should be noted that such giant jumps have never been observed in (sub-)micrometer-diameter superconducting cylinders.

Remarkably, in the presence of a magnetic field applied parallel to the cylinder axis, a hollow superconducting cylinder is a model of a bulk sample in SSS. At the same time, this object is free of the complications associated with the presence of the normal state in the sample bulk. Namely, if the external magnetic field H_{ext} increases slowly and the field in the cylinder hollow does not change, the current in the wall increases and can reach the critical value I_c . A further increase of H_{ext} makes the wall to transit to the normal state, with the order parameter equal to zero. An external magnetic field penetrates then into the hollow and the current in the wall decreases to zero. The normal state of the wall at $I = 0$ is unstable and superconductivity in the wall is restored. In the superconducting state, the total current in the wall is zero, since the magnetic fields inside and outside the cylinder are equal. Within the framework of the CSM, the ac susceptibility should exhibit *jumps* as a function of the amplitude of the external ac field H_{ac} . This prediction and a sharp increase in the loss for the ac amplitude near the critical field predicted in [19] have not yet been confirmed experimentally.

Here, we present the results of an experimental study of the low-frequency (128-8192 Hz) ac magnetic response of macroscopic thin-walled superconducting cylinders in superimposed dc and ac magnetic fields applied parallel to the cylinder axis. Distinct from the CSM predictions, our experiments reveal that the ac susceptibility χ is a *smooth* function of H_{ac} . For the explanation of our observations we propose a phenomenological model of partial penetration of magnetic flux (PPMF). The PPMF model implies that after a restoration of the superconducting state in the wall, the magnetic fields inside and outside the cylinder are not equal, and the value of the penetrating flux is random for each penetration. In this case χ is a smooth function of H_{ac} . The proposed PPMF model for the low-frequency ac response is in very good agreement with the experimental data for the first-harmonic ac susceptibility in the entire temperature range for arbitrary dc magnetic fields and ac excitation amplitudes. However, in a certain range of temperatures, the values of the physical parameters deduced within the framework of this model are questionable.

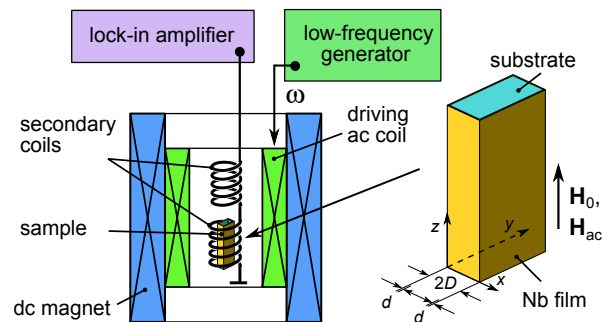


FIG. 2. Block-diagram of the experimental setup and the sample geometry. Both dc and ac magnetic fields are applied parallel to the cylinder axis.

II. SAMPLES AND SETUP

The samples are two thin-walled superconducting cylinders with a rectangular cross-section. The samples were prepared by dc magnetron sputtering of Nb on rotating sapphire substrates (Gavish Sapphire Products, Israel). The dimensions of the samples are $1.4 \times 3 \times 12 \text{ mm}^3$ (sample F15) and $1.4 \times 3 \times 21 \text{ mm}^3$ (sample GL). The wall thickness is 300 nm for sample F15 and it is 120 nm for sample GL.

The magnetic moment oscillations of the samples were measured at the first, second and third harmonics of the driving ac frequency using the pickup coils method [28]. The dc and ac magnetic fields were applied parallel to the long axis of the cylinders, see Fig. 2 for the geometry. The amplitude and phase of the imbalanced signal were measured with a lock-in amplifier. A homemade measurement cell of the experimental setup was adapted to a commercial SQUID magnetometer. The block diagram of the setup is shown in Fig. 2. The temperature dependences of the signals at the first, second and third harmonics of the excitation frequency were measured concurrently in two modes. In the temperature-sweep mode, temperature was swept at a rate of 0.1 K/min, with a continuous measurement of the magnetic response. The sweep rate 0.1 K/min was low enough to avoid a lag between the actual sample temperature and the temperature measured by the sensor, as confirmed experimentally. In the second mode, temperature was changed point-by-point, with temperature stabilization at each point. The amplitude H_{ac} of the ac magnetic field was 0.005-0.2 Oe. The second-harmonic signal was negligible, and we will not discuss its behavior here.

The ac magnetic moment of a sample in the ac magnetic field $H_{ext} = H_{ac} \exp(-i\omega t)$ is given by

$$M = V H_{ac} \sum \chi_n \exp(-in\omega t), \quad (1)$$

where V is the sample volume and $\chi_n = \chi_n(\omega, H_{ac})$ is the ac magnetic susceptibility at the n -th harmonic of the driving ac frequency ω . The ac field is shielded completely at low temperatures. This allows for the deduction of the absolute value of the in-phase and out-of-phase components of the ac magnetic susceptibility at all temperatures and magnetic fields.

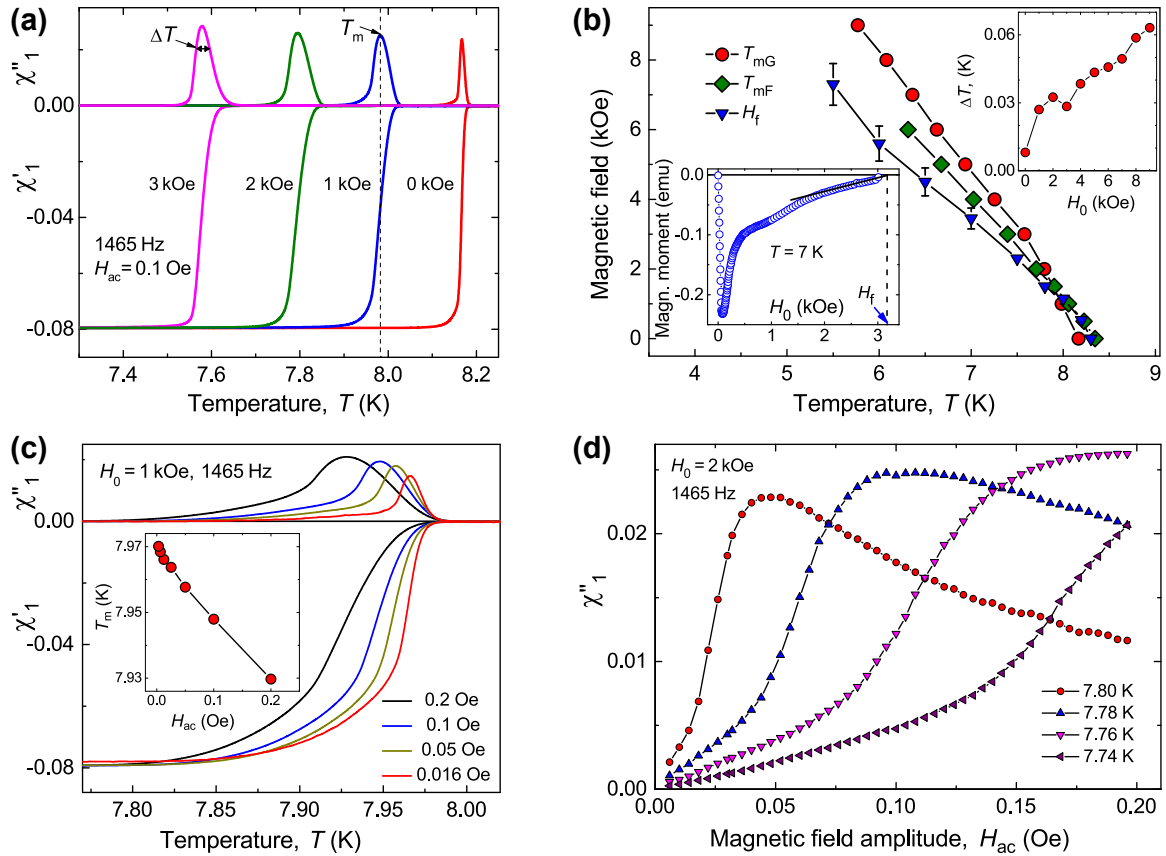


FIG. 3. (a) $\chi'_1(T)$ and $\chi''_1(T)$ for a series of dc field values for sample GL. T_m : temperature at the maximum of absorption; ΔT : linewidth of the absorption peak. (b) Dependence of T_m on the magnetic field and H_f on the temperature in the H - T plane. T_{mF} and T_{mG} are the T_m values for samples F15 and GL, respectively. Lower inset: Magnetization curve for sample F15. Upper inset: Field dependence of the linewidth ΔT for sample GL. (c) $\chi'_1(T)$ and $\chi''_1(T)$ for a series of excitation amplitudes for sample GL. Inset: T_m versus H_{ac} at $H_0 = 1$ kOe. (d) $\chi''_1(H_{ac})$ for a series of temperatures near $T_m = 7.76$ K for sample GL. The measurements were carried out in the swept temperature (a-c) and the point-by-point (d) modes.

III. EXPERIMENT

The experimentally measured dependences of the magnetic susceptibility as a function of temperature T , dc magnetic field magnitude H_0 and ac magnetic field amplitude H_{ac} are presented in Fig. 3. Here, χ'_1 and χ''_1 are real and imaginary parts of the complex ac susceptibility $\chi_1 = \chi'_1 + i\chi''_1$ measured at the first harmonics of the excitation frequency. The dependences $\chi'_1(T)$ and $\chi''_1(T)$ for sample GL are shown in Fig. 3(a) for a series of dc magnetic field magnitudes. With increase of H_0 , the absorption peak, with a maximum at the temperature T_m , shifts towards lower temperatures and its linewidth ΔT increases, see Fig. 3(b). Here, the linewidth ΔT was deduced at 70% of the maximal value of χ''_1 . We note that the linewidth $\Delta T_m < 0.02$ K in the investigated range of magnetic fields. This allows us to deduce the third critical field $H_{c3} = H_0|_{T=T_m}$ with high accuracy.

The total magnetic moment of a cylinder in a parallel dc magnetic field is determined by the difference between the magnetic field in the hollow and the applied external field, since the volume of the superconducting thin wall is very small. The lower inset in Fig. 3(b) shows an ascending branch

of the magnetization curve for sample F15, from where we deduce the dc magnetic field H_f at which the dc magnetic moment becomes equal to zero. Measurements of the magnetic moment of sample GL are impossible in our magnetometer for technical reasons. It should be noted that at $H_0 = H_f$ the internal dc magnetic field becomes equal to the external field. It can be assumed that $H_f = H_{c2}$, but the noise level near H_f is too high for an unambiguous conclusion. From Fig. 3(b) it is clear that the transition to the superconducting state in a non-zero magnetic field occurs at a higher temperature than the temperature determined by the $H_f(T)$ line. This means that the complete penetration of the dc magnetic field does not yet indicate a transition to the normal state.

The response of a thin-walled cylinder to an ac magnetic field is nonlinear. This means that there is no pure linear ac response of the sample near the transition to the normal state. Figure 3(c) shows how the excitation amplitude H_{ac} affects $\chi'_1(T)$ and $\chi''_1(T)$. An increase of H_{ac} leads to a broadening and a shift of the absorption peak towards lower temperatures. The decrease of T_m with increase of H_{ac} is shown in the inset in Fig. 3(c). The amplitude dependence of χ''_1 has a different character at slightly different temperatures, see Fig. 3(d). The

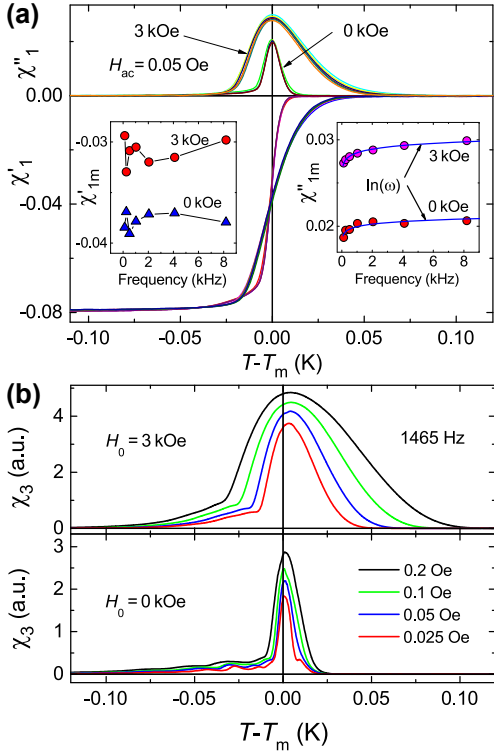


FIG. 4. (a) $\chi'_1(T)$ and $\chi''_1(T)$ at $H_0 = 0$ and 3 kOe for seven excitation frequencies in the range 128 – 8192 Hz for sample GL. Insets: Frequency dependences of χ'_1 and χ''_1 at $T = T_m$ for $H_0 = 0$ and 3 kOe. (b) $\chi_3(T)$ and $\chi_3(T)$ at $H_0 = 0$ and 3 kOe for a series of ac amplitudes for sample GL.

reasons for this behavior are the line broadening and the peak shift illustrated in Fig. 3(c).

In Fig. 4(a) we show the real and imaginary parts of χ_1 as a function of temperature for sample GL for seven frequencies from 128 to 8192 Hz and the ac amplitude 0.05 Oe in zero and 3 kOe dc magnetic fields. The respective frequency dependences of χ'_1 and χ''_1 at $T = T_m$ are shown in the insets in Fig. 4(a). The frequency dispersion of χ'_1 is negligible. However, there is a weak frequency dispersion $\chi''_1(\omega) \propto \ln(\omega)$.

Figure 4(b) presents the magnitude of the susceptibility at the third harmonics of the ac driving frequency, $\chi_3(T)$, for a series of ac amplitudes at two dc magnetic field values. We do not observe zeroing of the third-harmonic signal with decrease of the ac amplitude. An analysis of the experimental data shows that the perturbation theory is not applicable to the third-harmonic signal. It should be noted that a strictly linear ac response near the transition to the normal state does not exist in bulk samples, as was demonstrated in Ref. [29].

IV. THEORETICAL MODEL

A. Two-fluid model

As a model for our samples we consider an infinite dielectric slab of thickness $2D$ with superconducting films of thick-

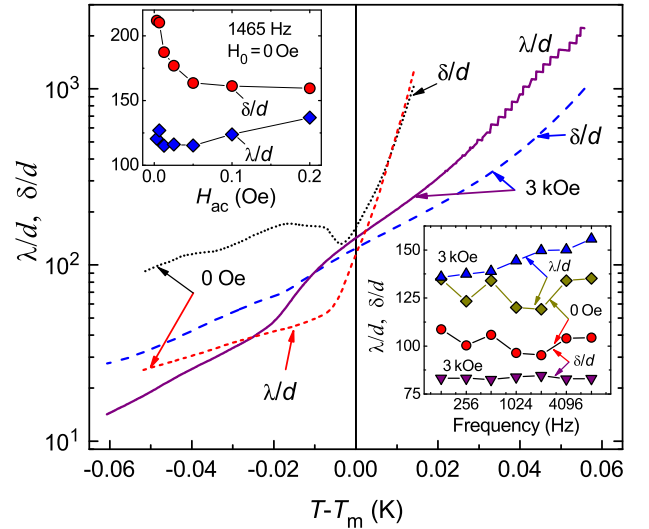


FIG. 5. Temperature dependence of λ/d and δ/d in zero and 3 kOe dc magnetic field at a frequency of 1465 Hz and $H_{ac} = 0.05$ Oe. Upper inset: Amplitude dependence of λ/d and δ/d at $T = T_m$. Lower inset: λ/d and δ/d versus frequency at $T = T_m$.

ness d on both surfaces of the slab and the condition $D \gg d$, see Fig. 2. The dc and ac magnetic fields are applied along the z -axis which is parallel to the cylinder axis. Within the framework of the two-fluid model and neglecting any nonlinear effects, for the current density $j(\omega)$ and the vector potential $A(\omega)$ in the superconducting film we take the following equations [10]

$$j(\omega) = -\frac{c}{4\pi} \left[\frac{1}{\lambda^2(\omega)} - \frac{2i}{\delta^2(\omega)} \right] A(\omega) \equiv -\frac{c}{4\pi\tilde{\lambda}^2} A(\omega),$$

$$\frac{d^2 A(\omega)}{dx^2} = -\frac{4\pi}{c} j(\omega). \quad (2)$$

In Eq. (2), the parameters $\lambda(\omega)$ and $\delta(\omega)$ characterize the effective penetration length and the skin depth of the magnetic field in the film due to the superconducting and normal components of the conductivity. The axis x is chosen perpendicular to the slab, as shown in Fig. 2. The solution of Eq. (2) yields the magnetic field inside the slab

$$\frac{h_{in}}{h_{ext}} = \frac{1}{[\cosh(d/\tilde{\lambda}) + (D/\tilde{\lambda}) \sinh(d/\tilde{\lambda})]}. \quad (3)$$

Equation (3) permits to calculate the susceptibility χ_1 of the slab. Inverting Eq. (3) one can find λ and δ from the experimental data for χ_1 at a given amplitude and frequency of the ac excitation. The results of this procedure are presented in Fig. 5. For this plot, we used the experimental data obtained for sample GL at a frequency of 1465 Hz and $H_{ac} = 0.05$ Oe at zero and 3 kOe dc magnetic fields.

The first thing to note is the large values of λ/d and δ/d just above T_m . During the transition δ/d decreases approximately by 10 times that corresponds to an increase of the dissipative conductivity by 100 times if one uses the standard ex-

pression for the normal skin-effect. Since the relaxation time of normal electrons is very short, $\omega\tau \ll 1$, the frequency dispersion of the conductivity of such electrons is negligible at low frequencies, so that δ should be $\propto 1/\sqrt{\omega}$. However, there is no signatures of $\delta \propto \sqrt{\omega}$ (lower inset in Fig. 5). These data demonstrate the accuracy of the quasilinear approach. For a linear system its parameters do not depend on the amplitude of the external field. These results indicate that the observed $\chi_1''(\omega)$ is not directly related to the presence of the normal phase. The amplitude dependences of λ/d and δ/d at $T = T_m$ are shown in the upper inset of Fig. 5. It should be noted that the results for λ/d and δ/d given above were obtained in the linear approximation and they give only estimates for λ/d and δ/d . The large values of λ/d and δ/d obtained within the framework of the two-fluid model make a more general Ginzburg-Landau approach desirable.

B. Ginzburg-Landau approach

The Ginzburg-Landau equations for the order parameter and the vector-potential in the film read

$$\frac{d^2 f}{\kappa^2 dx^2} - (\tilde{a} - k)^2 f + \frac{\xi_0^2}{\xi^2(T)} f - f^3 = 0, \quad (4)$$

$$\frac{d^2 \tilde{a}}{dx^2} - f^2 (\tilde{a} - k) = 0,$$

with the order parameter $\psi = f(x)\psi_0 \exp(iky)$, where ψ_0 is the order parameter and ξ_0 is the coherence length at arbitrary chosen temperature T_0 . The dimensionless variables in Eq. (4) are the vector-potential $\tilde{a} = 2e\xi_0 A/\hbar c$, magnetic field $h = 2e\xi_0 dH/\hbar c = 2\pi\xi_0 dH/\phi_0$, ϕ_0 is the flux quantum, κ is the Ginzburg-Landau parameter, $x = x/\lambda_0$ is the dimensionless coordinate, λ_0 is London's penetration length at T_0 . The chosen gauge is $\tilde{a} = 0$ in the center of the slab. In these variables, the second critical magnetic field reads $h_{c2} = \kappa\xi_0^2/\xi(T)$. The parameter k determines the magnetic field inside the slab. Namely, $k = h_{ext}(D + d/2)$ corresponds to the inside field equal to the external field, $h_{int} = h_{ext}$. The transition to the superconducting state corresponds to a change of the parameter $gg = \xi_0^2/\xi^2(T) = (T_c - T)/(T_c - T_0)$ from zero to a certain final value. In the following we assume that the temperature T_0 was chosen from the condition $\lambda(T_0) = d$ at $\kappa = 4$, and $D/d = 6250$.

A numerical solution of Eqs. (4) reveals that the order parameter $f(x)$ in low magnetic fields weakly depends on x and it has a maximum in the middle of the film. At the same time, from the solutions of Eqs. (4) follows that the superconducting state for a given magnetic field inside the slab (i.e., for a given k) can exist only in a narrow interval of external magnetic fields $|h_{ext} - h_{int}| < h_c$. An increase of the external field outside this interval leads to an abrupt decrease of the order parameter to zero. The range of external magnetic fields, where the maximal order parameter f_m differs from zero, decreases rapidly with the ratio D/d . Figure 6 shows the dependence of f_m on the external magnetic field for two ratios D/d . It can be seen from Fig. 6(a) that h_c sharply decreases with increase

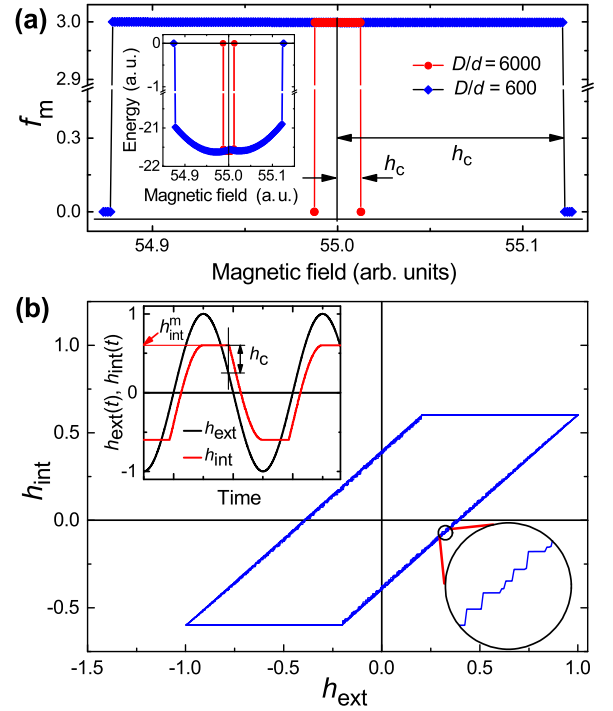


FIG. 6. (a) Field dependence of the maximal superconducting order parameter f_m for two D/d ratios. Inset: Field dependence of the energy of the system for two values of D/d . (b) $h_{int}(h_{ext})$ during a slow course of 10 ac cycles. Zoom: tiny jumps of $h_{int}(h_{ext})$ in a part of a single ac cycle. Inset: Waveform of the ac magnetic fields h_{ext} and h_{int} .

of the ratio D/d . The inset in Fig. 6(a) shows how the energy of the system depends on the magnetic field. The energy has two minima, which correspond to SSS on opposite sides of the film.

This abrupt destruction of the superconducting state is completely analogous to the well-known current-induced breakdown of the superconducting state in thin films [30]. However, the value of the critical current for a cylinder is much smaller. The critical magnetic field h_c characterizes the maximum possible difference between the external and internal magnetic fields. At the same time, this quantity determines the value of the total critical current. Numerical calculations reveal that $h_c \propto (T_c - T)^{1/2}$ for a cylinder while for a thin film with thickness $d \ll \xi$, the critical current $j_c \propto (T_c - T)^{3/2}$ [30].

C. Partial penetration of magnetic flux model

The obtained solution of the Ginzburg-Landau equations shows that the value of the critical field of a thin-walled cylinder is very small. Therefore, the ac magnetic field of a small amplitude can destroy the superconducting state. The experiment reveals that the frequency dispersion of the ac response is very small, see Fig. 4(a), and therefore a quasistatic approach can be applied for the description of the ac response. In this case, application of the critical state model leads to

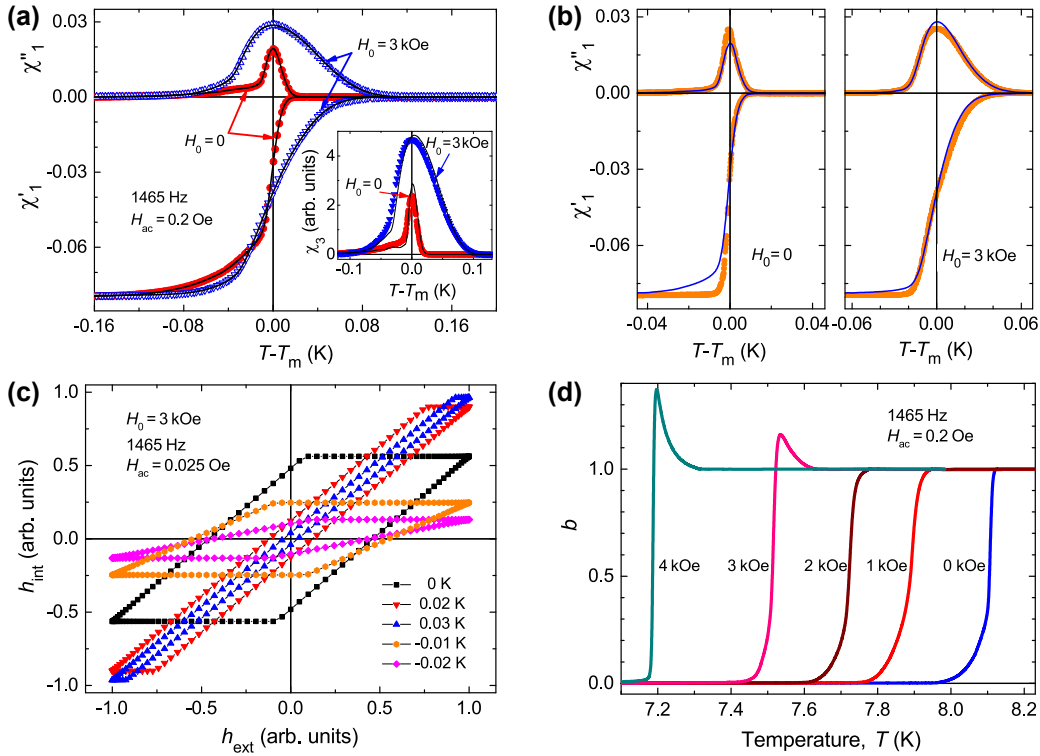


FIG. 7. (a) $\chi_1''(T)$ and $\chi_1'(T)$ (main panel) and $\chi_3(T)$ (inset) at zero and 3 kOe magnetic fields. Lines: experiment; symbols: fits. (b) $\chi_1''(T)$ and $\chi_1'(T)$ for $b = 1$ at zero and 3 kOe magnetic fields. Lines: experiment; symbols: fits. (c) Evolution of the $h_{int}(h_{ext})$ dependence with the temperature difference ($T - T_m$), as indicated in the legend. (d) Temperature dependences of the parameter b for a series of dc magnetic fields. In all panels, the measurements were carried out in the temperature-sweep mode. In all panels, the shown data are for sample GL.

the following scenario of the penetration of an ac field into a thin-walled cylinder. The ac component of the magnetic field $h_{ext} = h_0 + h_{ac} \sin(\omega t)$ does not penetrate into the slab if $h_{ac} < h_c$. However, if $h_{ac} \sin(\omega t) > h_c$ at some time t , then SSS becomes unstable, a transition to the normal state occurs, and the field penetrates into the slab. However, since $T < T_c$, the normal state is unstable and the superconducting state is restored with a new value of k , which corresponds to an increased internal field. If full penetration occurs, the internal field becomes equal to the external one. In such a model, one can expect the appearance of jumps in the ac susceptibility as a function of the excitation amplitude. These features have not been confirmed experimentally.

At the same time, there is another possibility related to a partial penetration of the external magnetic field. Namely, after the restoration of superconductivity, the internal field does not reach the value of the external field, and the difference between the external and internal fields $|h_{ext} - h_{int}|/h_c$ is a random variable between 0 and 1. Within the framework of this model we obtain the internal magnetic field h_{int} as a function of the instant value of the external field $h_{ext} = h_{ac} \sin(\omega t)$ in a form similar to that postulated in [2] for discussing the ac response of bulk superconductors in SSS. In the case of PPMF, the $h_{int}(h_{ext})$ loop during a slow passage of 10 ac cycles looks as shown in Fig. 6(b). The inset in Fig. 6(b) shows the $h_{int}(h_{ext})$ in a part of one ac cycle. The main difference between the CSM [2] and the PPMF model considered here

is that in the first model, Fig. 1, the field penetrates smoothly, and in the PPMF model, Fig. 6(b), small jumps are formed. It should be noted that a swept dc field can also penetrate into a thin-walled superconducting niobium cylinder in the form of giant jumps [27]. The presence of small jumps leads to the appearance of an excess noise at high frequencies, but this weakly affects the response at low frequencies, due to the fact that the ac response is measured with a lock-in amplifier which averages the signal over at least a hundred of ac cycles. After averaging over small jumps, the loop $h_{int} = h_{int}(h_{ext})$, Fig. 6(b), can be characterized by two main free parameters: (1) $a = h_{int}^m/h_{ac}$, where h_{int}^m is the maximal value of h_{int} , see the inset in Fig. 6(b), and (2) the average slope of the inclined part of the $h_{int}(h_{ext})$ loop, $b = dh_{int}/dh_{ext}$. For the critical state model [2] and the model suggested here the parameter $b = 1$.

V. DISCUSSION

The relation between the internal and external magnetic fields obtained within the framework of the PPMF model should now be employed for fitting the experimentally measured dependences of the magnetic susceptibility on temperature, dc magnetic field value and amplitude of excitation. To accomplish this, one proceeds as follows. First, after averaging the minor magnetization loop over small jumps, one obtains the waveform of $h_{int}(t)$ as shown in the inset of Fig. 6(b).

Next, by performing the Fourier transform $h_{int}(t)$, the in-phase and out-of-phase components of the ac susceptibility can be obtained as a function of the parameters a and b . Finally, by varying a and b as fitting parameters, it is possible to completely fit the experimental data for $\chi_1(T)$ near the superconducting transition at any temperature point. The result of the fitting procedure is shown in Fig. 7(a). One can see that the fits are in excellent agreement with the experimental data.

The parameters a and b obtained from fitting of χ_1 can be used for the calculation of χ_3 . The criterion for this calculation is the equality of the areas under the experimental and calculated curves. The calculation result is shown in the inset in Fig. 7(a). It turns out that the third harmonics of $h_{int}(h_{ext}, a, b)$ with a and b obtained from the above mentioned procedure does not fit very well to the measured $\chi_3(T)$ dependences. Yet, the overall behavior of $\chi_3(T)$ is reproduced quite well. It should be noted that the $h_{int}(h_{ext})$ dependence with the parameter $b = 1$ can also be used for fitting of the experimental data. As an example, in Fig. 7(b) we show the best fits with only one free parameter a . Having a larger discrepancy at the foot of the superconducting transition, these fits are not so good as the two-parameter fits.

The performed calculations with the two fitting parameters allow us to plot the $h_{int}(h_{ext})$ dependence at any temperature in the temperature range where χ_1'' is nonzero. The shape of the $h_{int}(h_{ext})$ dependence changes with temperature, as shown in Fig. 7(c). It can be seen from Fig. 7(c) that the parameters a and b change with temperature. It is natural that in the normal state the parameters $a = 1$ and $b = 1$ since in the normal state $h_{int} = h_{ext}$. Deeply in the superconducting state, the parameter a turns to zero since $h_{int} = \text{const}$. The behavior of the parameter b is more complicated. Figure 7(d) shows the temperature dependence of the parameter b for a series of dc magnetic fields values. In addition, when $H_0 > 2$ kOe, the parameter b near T_m exceeds 1. It turns out that the peak magnitude increases with increasing excitation amplitude.

Finally, using the experimental data, it is possible to plot the critical field $H_c = h_c H_{ac}$ as a function of the external parameters such as temperature and excitation amplitude. Here, H_{ac} is the amplitude of the applied ac magnetic field in Oe and $h_c \equiv (1 - a)$ is defined within the framework of the PPMF model. Figure 8(a) shows the temperature dependences of the critical field $H_c(T)$ and $\chi_1''(T)$ at a magnetic field of 2 kOe for ac amplitudes of 0.196, 0.1, and 0.052 Oe. The imaginary part of the ac susceptibility was measured at $H_{ac} = 0.196$ Oe. The measurements were carried out in the point-by-point mode with decreasing temperature. This figure shows that H_c increases with decreasing temperature and it saturates at sufficiently low temperatures. Note that the calculation of H_c is meaningful when $H_c < H_{ac}$ and at sufficiently low temperatures H_c becomes greater than H_{ac} . We have to mention that the calculation of the parameters of the $h_{int}(h_{ext})$ loops, and then H_c , is only possible if both χ_1' and χ_1'' are not equal to zero. However, at low temperatures $\chi_1'' = 0$. At high temperatures, $H_c(T)$ is a quadratic rather than a linear function of temperature, as one might expect. In Fig. 8(b) we show the amplitude dependences of $H_c(H_{ac})$ at constant temperatures near the absorption peak. It is seen that at $T \geq T_m$, H_c reaches

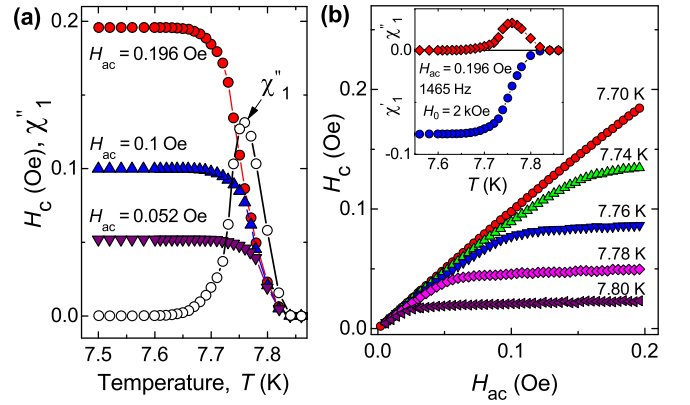


FIG. 8. (a) Temperature dependence of the critical magnetic field H_c for three excitation amplitudes and $5 \times \chi_1''(T)$ at $H_{ac} = 0.196$ Oe. (b) Amplitude dependence of H_c at temperatures near the absorption peak, $T_m = 7.76$ K at $H_{ac} = 0.196$ Oe. Inset: Temperature dependences of χ_1' and χ_1'' at $H_0 = 2$ kOe and $H_{ac} = 0.196$ Oe. In both panels, the measurements were carried out in the point-by-point mode.

a plateau, i.e. ceases to depend on H_{ac} , and as the temperature decreases, the plateau is reached at higher amplitudes. Hence, one can conclude that the calculations of H_c are reliable only at $T \geq T_m$ in the plateau region.

In all, the $h_{int}(h_{ext})$ loops calculated within the framework of the PPMF model are in good agreement with the experimental data in the entire temperature range where both χ_1' and χ_1'' are nonzero, see Fig. 7(a). However, it is impossible to conclude that this model fully describes the experiment for any dc fields and excitation amplitudes, since there is a region of fields and temperatures where the parameter $b \neq 1$. Note that $b > 1$ means that the change in the internal field is larger than that of the external one. However, for $T > T_m$, the parameters a and b of the dependences $h_{int}(h_{ext})$ are reasonable and the model of the $h_{in}(h_{ext})$ loops is fully applicable.

As a final comment, the transition in a dc magnetic field occurs near the $H_{c3}(T)$ line. To describe the transition in a dc magnetic field, vortices must be taken into account. The nucleation problem of the superconducting phase in a plate with a parallel magnetic field was solved long ago in the linear Ginzburg-Landau approximation [31]. The solution was applied to explain the reentrance of superconductivity in strong magnetic fields by stopping the movement of vortices due to the appearance of a superconducting surface sheath [32]. A strong pinning of vortices with a reentrant superconducting state was also observed in a superconducting/semiconductor superlattices in the presence of magnetic fields applied parallel to the layers [33]. It can be assumed that the low-frequency dynamics of vortices in the plate near H_{c3} can explain our experimental data. However, stopping the vortex motion near H_{c3} will result in a splitting of the field dependence χ_1'' , but we did not observe such a splitting either in the present or in our previous experiments [34, 35].

VI. CONCLUSION

This paper presents the results of an experimental study of the ac response of thin-walled hollow superconducting cylinders in the course of transition to the superconducting state when both ac and dc magnetic fields are parallel to the cylinder axis. While the critical state model asserts that the susceptibility χ should exhibit jumps as a function of the external ac field amplitude H_{ac} , because of the periodic destruction and restoration of the surface superconducting state in the cylinder wall, our experiments reveal that χ is a smooth function of H_{ac} . For the explanation of our observations we have proposed a phenomenological model of partial penetration of magnetic flux. This model implies that after a restoration of the superconducting state, the magnetic fields inside and outside the cylinder are not equal, and the value of the penetrating

flux is random for each penetration. In this case χ is a smooth function of H_{ac} and the model of minor magnetization loops, $h_{int}(h_{ext})$, fits very well to the experimental data on the temperature dependence of the signal of the first harmonics at any dc magnetic fields and excitation amplitudes. However, in a certain temperature range the values of physical parameters deduced within the framework of the model should be treated with care.

ACKNOWLEDGEMENTS

We thank Yu. A. Genenko and G. I. Leviev for helpful discussions. Support by the European Cooperation in Science and Technology via COST Action CA16218 (NANOCOBY-BRI) is gratefully acknowledged. Financial support of the grant agency VEGA 2/0117/18 and APVV 19-0303 are kindly appreciated.

-
- [1] E. Maxwell and M. Strongin, *Phys. Rev. Lett.* **10**, 212 (1963).
 - [2] R. W. Rollins and J. Silcox, *Phys. Rev.* **155**, 404 (1967).
 - [3] J. R. Hopkins and D. K. Finnemore, *Phys. Rev. B* **9**, 108 (1974).
 - [4] T. Ishida and R. B. Goldfarb, *Phys. Rev. B* **41**, 8937 (1990).
 - [5] F. Gömöry, *Supercond. Sci. Technol.* **10**, 523 (1997).
 - [6] A. Youssef, Z. Svindrych, and Z. Janu, *J. Appl. Phys.* **106**, 063901 (2009).
 - [7] P. R. Doidge and K. Sik-Hung, *Phys. Lett.* **12**, 82 (1964).
 - [8] G. D. Cody and R. E. Miller, *Phys. Rev.* **173**, 481 (1968).
 - [9] A. F. Khoder, *Phys. Lett. A* **94**, 378 (1983).
 - [10] M. Tinkham, *Introduction to Superconductivity* (Mineola, New York, 2004).
 - [11] M. Strongin, A. Paskin, D. G. Schweitzer, O. F. Kammerer, and P. P. Craig, *Phys. Rev. Lett.* **12**, 442 (1964).
 - [12] M. I. Tsindlekht, I. Felner, M. Zhang, A. F. Wang, and X. H. Chen, *Phys. Rev. B* **84**, 052503 (2011).
 - [13] A. A. Abrikosov, *J. Exp. Theor. Phys.* **20**, 480 (1965).
 - [14] H. J. Fink, *Phys. Rev. Lett.* **14**, 309 (1965).
 - [15] J. G. Park, *Phys. Rev. Lett.* **15**, 352 (1965).
 - [16] H. J. Fink, *Phys. Rev. Lett.* **16**, 447 (1966).
 - [17] H. J. Fink, *Phys. Rev.* **177**, 732 (1969).
 - [18] H. J. Fink, *Phys. Rev.* **161**, 417 (1967).
 - [19] Y. Mawatari, *Phys. Rev. B* **83**, 134512 (2011).
 - [20] R. O. Rezaev, E. I. Smirnova, O. G. Schmidt, and V. M. Fomin, *Commun. Phys.* **3**, 144 (2020).
 - [21] V. N. Gladilin, J. Tempere, J. T. Devreese, and V. V. Moshchalkov, *Phys. Rev. B* **86**, 104508 (2012).
 - [22] V. M. Fomin, R. O. Rezaev, and O. G. Schmidt, *Nano Letters, Nano Lett.* **12**, 1282 (2012).
 - [23] R. Córdoba, A. Ibarra, D. Mailly, and J. M. De Teresa, *Nano Lett.* **18**, 1379 (2018).
 - [24] C. Qiu and T. Qian, *Phys. Rev. B* **79**, 054513 (2009).
 - [25] M. Lu-Dac and V. V. Kabanov, *Phys. Rev. Lett.* **105**, 157005 (2010).
 - [26] R. O. Rezaev, E. A. Levchenko, and V. M. Fomin, *Supercond. Sci. Technol.* **29**, 045014 (2016).
 - [27] M. I. Tsindlekht, V. M. Genkin, I. Felner, F. Zeides, N. Katz, Š. Gazi, and Š. Chromik, *Physica C* **529**, 1 (2016).
 - [28] G. I. Leviev, V. M. Genkin, M. I. Tsindlekht, I. Felner, Y. B. Paderno, and V. B. Filippov, *Phys. Rev. B* **71**, 064506 (2005).
 - [29] M. I. Tsindlekht, V. M. Genkin, G. I. Leviev, I. Felner, O. Yuli, I. Asulin, O. Millo, M. A. Belogolovskii, and N. Y. Shitsevalova, *Phys. Rev. B* **78**, 024522 (2008).
 - [30] P. G. De Gennes, *Superconductivity of metals and alloys* (W.A. Benjamin, INC, New York, 1966).
 - [31] D. Saint-James, G. Sarma, and E. J. Thomas, *Type II superconductivity* (Pergamon Press, Oxford-London-Edinburg-New York-Toronto-Sydney-Paris-Braunschweig, 1969).
 - [32] R. Córdoba, T. I. Baturina, J. Sesé, A. Yu Mironov, J. M. De Teresa, M. R. Ibarra, D. A. Nasimov, A. K. Gutakovskii, A. V. Latyshev, I. Guillamón, H. Suderow, S. Vieira, M. R. Baklanov, J. J. Palacios, and V. M. Vinokur, *Nat. Commun.* **4**, 1437 (2013).
 - [33] O. V. Dobrovolskiy, V. M. Bevez, M. Y. Mikhailov, O. I. Yuzepovich, V. A. Shklovskij, R. V. Vovk, M. I. Tsindlekht, R. Sachser, and M. Huth, *Nat. Commun.* **9**, 4927 (2018).
 - [34] M. I. Tsindlekht, V. M. Genkin, I. Felner, F. Zeides, and N. Katz, *Phys. Rev. B* **90**, 014514 (2014).
 - [35] M. I. Tsindlekht, V. M. Genkin, I. Felner, F. Zeides, N. Katz, Š. Gazi, Š. Chromik, O. V. Dobrovolskiy, R. Sachser, and M. Huth, *J. Phys.: Cond. Matt.* **28**, 215701 (2016).